Two-Phase Heat Transfer

Mizra Mohammed Shah

ASME PRESS

WILEY

Two-Phase Heat Transfer

Wiley-ASME Press Series

Advanced Multifunctional Lightweight Aerostructures: Design, Development, and Implementation
Kamran Behdinan and Rasool Moradi-Dastjerdi

Vibration Assisted Machining: Theory, Modelling and Applications
Lu Zheng, Wanqun Chen, Dehong Huo

Two-Phase Heat Transfer
Mirza Mohammed Shah

Computer Vision for Structural Dynamics and Health Monitoring
Dongming Feng, Maria Q Feng

Theory of Solid-Propellant Nonsteady Combustion
Vasily B. Novozhilov, Boris V. Novozhilov

Introduction to Plastics Engineering
Vijay K. Stokes

Fundamentals of Heat Engines: Reciprocating and Gas Turbine Internal Combustion Engines
Jamil Ghojel

Offshore Compliant Platforms: Analysis, Design, and Experimental Studies
Srinivasan Chandrasekaran, R. Nagavinothini

Computer Aided Design and Manufacturing
Zhuming Bi, Xiaoqin Wang

Pumps and Compressors
Marc Borremans

Corrosion and Materials in Hydrocarbon Production: A Compendium of Operational and Engineering Aspects
Bijan Kermani and Don Harrop

Design and Analysis of Centrifugal Compressors
Rene Van den Braembussche

Case Studies in Fluid Mechanics with Sensitivities to Governing Variables
M. Kemal Atesmen

The Monte Carlo Ray-Trace Method in Radiation Heat Transfer and Applied Optics
J. Robert Mahan

Dynamics of Particles and Rigid Bodies: A Self-Learning Approach
Mohammed F. Daqaq

Primer on Engineering Standards, Expanded Textbook Edition
Maan H. Jawad and Owen R. Greulich

Engineering Optimization: Applications, Methods and Analysis
R. Russell Rhinehart

Compact Heat Exchangers: Analysis, Design and Optimization using FEM and CFD Approach
C. Ranganayakulu and Kankanhalli N. Seetharamu

Robust Adaptive Control for Fractional-Order Systems with Disturbance and Saturation
Mou Chen, Shuyi Shao, and Peng Shi

Robot Manipulator Redundancy Resolution
Yunong Zhang and Long Jin

Stress in ASME Pressure Vessels, Boilers, and Nuclear Components
Maan H. Jawad

Combined Cooling, Heating, and Power Systems: Modeling, Optimization, and Operation
Yang Shi, Mingxi Liu, and Fang Fang

Applications of Mathematical Heat Transfer and Fluid Flow Models in Engineering and Medicine
Abram S. Dorfman

Bioprocessing Piping and Equipment Design: A Companion Guide for the ASME BPE Standard
William M. (Bill) Huitt

Nonlinear Regression Modeling for Engineering Applications: Modeling, Model Validation,
and Enabling Design of Experiments
R. Russell Rhinehart

Geothermal Heat Pump and Heat Engine Systems: Theory and Practice
Andrew D. Chiasson

Fundamentals of Mechanical Vibrations
Liang-Wu Cai

Introduction to Dynamics and Control in Mechanical Engineering Systems
Cho W.S. To

Two-Phase Heat Transfer

Mirza Mohammed Shah

This Work is a co-publication between John Wiley & Sons Ltd and ASME Press.

This Work is a co-publication between John Wiley & Sons Ltd and ASME Press.

Registered Office(s)
John Wiley & Sons, Inc., 111 River Street, Hoboken, NJ 07030, USA
John Wiley & Sons Ltd, The Atrium, Southern Gate, Chichester, West Sussex, PO19 8SQ, UK

Editorial Office
The Atrium, Southern Gate, Chichester, West Sussex, PO19 8SQ, UK

For details of our global editorial offices, customer services, and more information about Wiley products visit us at www.wiley.com.

Wiley also publishes its books in a variety of electronic formats and by print-on-demand. Some content that appears in standard print versions of this book may not be available in other formats.

Library of Congress Cataloging-in-Publication Data Applied for:
9781119618614 (Hardback)

Cover Design: Wiley
Cover Image: © Jub Rubjob/Getty Images

Set in 9.5/12.5pt STIXTwoText by SPi Global, Chennai, India

10 9 8 7 6 5 4 3 2 1

Contents

Preface

The two-phase systems covered in this book include boiling, condensation, gas–liquid mixtures, and gas–solid mixtures. While there are many books on these topics, most of them are concerned mainly with theoretical aspects while information of practical use is addressed only briefly. The very few books that were intended to help the practicing engineers are greatly out of date. I therefore felt that there was a need for an up-to-date book that emphasized the practical aspects while also addressing the theoretical bases. This book is intended to fulfil this need.

The emphasis in this book is on information that is of practical use. For this reason, theories and methods that do not provide useable and adequately verified solutions are dealt only briefly though sufficient references are provided for more information about them. Effort has been made to provide a review of the state-of-art and the best available information for the design of a wide variety of heat exchangers in a clear and concise manner. This information includes experimental data, theoretical solutions, and empirical correlations. Accuracy and range of applicability of formulas/correlations presented is stated. Clear recommendations are made for application of the methods presented. A very wide variety of heat exchangers and applications is covered. These include boiling and condensation of pure fluids and their mixtures in tubes and tube bundles, plate heat exchangers of various types, falling film heat exchangers, coils, bends, heat pipes, cryogenic pipelines, surfaces cooled by jets, mist cooling, rotating surfaces, spheres, disks, cones, etc. Boiling and condensation of metallic fluids is also discussed. Also included are heat exchangers with two-component gas–liquid mixtures, fluidized beds, and flowing gas–solid mixtures. As space travel and colonization are of much current interest, available information on effects of low gravity has been addressed.

While this book is primarily intended to assist practicing engineers and researchers, it may also be used as textbook for courses on two-phase heat transfer.

Finally, I thank Dr. Milaz Darzi for his help in getting some of the publications studied during the preparation of this book.

Redding, CT *Mirza Mohammed Shah*
11 April 2020

1

Introduction

1.1 Scope and Objectives of the Book

The two-phase systems covered in this book include boiling, condensation, gas–liquid mixtures, and gas–solid mixtures.

Two-phase heat transfer is involved in numerous applications. These include heat exchangers in refrigeration and air conditioning, conventional and nuclear power generation, solar power plants, aeronautics, chemical processes, petroleum industry, etc. In recent years, there has been increasing use of miniature heat exchangers for computers and other electronic intensive products.

The emphasis in this book is on information that is of practical use. For this reason, theories and methods that do not provide useable and adequately verified solutions are dealt only briefly though sufficient references are provided for more information about them. Effort is made to provide the best available information for the design of a wide variety of heat exchangers in a clear and concise manner. This information includes experimental data, theoretical solutions, and empirical correlations. Accuracy and range of applicability of formulas/correlations presented is stated. Clear recommendations are made for application of the methods presented. A very wide variety of heat exchangers is covered. These include boiling and condensation in tubes and tube bundles, plate heat exchangers of various types, falling film heat exchangers, coils, surfaces cooled by jets, mist cooling, rotating surfaces (tubes, disks, cones, etc.), spheres, etc. Boiling and condensation of metallic fluids is discussed besides those of non-metallic fluids. Also included are heat exchangers with two-component gas–liquid mixtures, fluidized beds, and flowing gas–solid mixtures.

In this chapter, information is provided that is needed for understanding and using the material in other chapters as well as in other publications. This includes explanation of commonly used terms, various models used in solving two-phase flow and heat transfer problems, distinction between minichannels and conventional channels, flow patterns and their prediction, etc. While the focus of this book is on two-phase heat transfer, methods for calculation of single-phase heat transfer, void fraction and pressure drop have also been briefly discussed as these are needed in the design of heat exchangers. References to sources for more information on these topics have been provided.

Only Newtonian fluids are considered in this book. All discussions pertain to non-metallic fluids except where stated otherwise.

1.2 Basic Definitions

Some commonly used terms are explained in the following.

Mass flux or mass velocity is the mass flow rate per unit area. It is usually designated as G. If W be the mass flow rate $\mathrm{kg\,s^{-1}}$ in a tube of cross-sectional area A_c ($\mathrm{m^2}$), $G = W/A_c$ ($\mathrm{kg\,m^{-2}\,s^{-1}}$).

Void fraction is the part of the total volume occupied by the gas phase. Consider a gas–liquid mixture flowing in a pipe. If A_L is the flow area occupied by liquid and A_G is the flow area occupied by gas, void fraction α is

$$\alpha = \frac{A_G}{A_L + A_G} = \frac{A_G}{A_c} \tag{1.2.1}$$

Liquid holdup R_L is the part of flow area occupied by liquid phase.

$$R_L = 1 - \alpha \tag{1.2.2}$$

Quality, usually given the symbol x, is mass flow rate of vapor divided by the total flow rate. With W_L as the flow rate of liquid and W_G that of gas,

$$x = \frac{W_G}{W_L + W_G} \tag{1.2.3}$$

Two types of phase velocities are used, actual, and superficial. The actual velocity of gas phase u_G is that in the area occupied by the gas phase:

$$u_G = \frac{W_G}{\rho_g A_c \alpha} = \frac{Gx}{\rho_g \alpha} \tag{1.2.4}$$

Two-Phase Heat Transfer, First Edition. Mirza Mohammed Shah.

where ρ_g is the density of gas. The actual liquid velocity is similarly defined and is given by

$$u_L = \frac{W_L}{\rho_L A_c(1-\alpha)} = \frac{G(1-x)}{\rho_f(1-\alpha)} \tag{1.2.5}$$

Superficial gas velocity u_{GS} is the velocity assuming that gas alone is flowing through the entire flow area. In other words, liquid is assumed to be absent. Then,

$$u_{\text{GS}} = \frac{W_G}{\rho_g A_c} = \frac{Gx}{\rho_g} \tag{1.2.6}$$

Similarly, superficial liquid velocity u_{LS} is defined as

$$u_{\text{LS}} = \frac{W_L}{\rho_L A_c} = \frac{G(1-x)}{\rho_f} \tag{1.2.7}$$

The superficial gas and liquid velocities are also called volumetric gas and liquid flux represented by the symbols j_G and j_L, respectively.

Gas and liquid velocities are often not equal. The difference in phase velocities $(u_G - u_L)$ is called the slip velocity, while u_G/u_L is known as slip ratio. The latter is expressed by the following relation obtained using Eqs. (1.2.4) and (1.2.5):

$$\frac{u_G}{u_L} = \left(\frac{x}{1-x}\right)\left(\frac{1-\alpha}{\alpha}\right)\left(\frac{\rho_f}{\rho_g}\right) \tag{1.2.8}$$

The relative velocity between phases u_{GL} can be written as

$$u_{\text{GL}} = (u_G - u_L) = \frac{j_G}{\alpha} - \frac{j_L}{(1-\alpha)} \tag{1.2.9}$$

The drift flux j_{GL} is defined as

$$j_{\text{GL}} = u_{\text{GL}}\alpha(1-\alpha) = j_G - \alpha j \tag{1.2.10}$$

where

$$j = j_{\text{GS}} + j_{\text{LS}} \tag{1.2.11}$$

The drift velocity of gas u_{Gj} with respect to a plane moving at a velocity j is defined as

$$u_{\text{Gj}} = u_G - j \tag{1.2.12}$$

The drift velocity of the liquid phase is

$$u_{\text{Lj}} = u_L - j \tag{1.2.13}$$

Heat flux, usually represented as q, is defined as the heat applied to a surface per unit area per unit time. If Q Watts are applied to a tube of diameter D and length L,

$$q = \frac{Q}{\pi DL} \tag{1.2.14}$$

In boiling systems, quality is usually defined assuming thermodynamic equilibrium between vapor and liquid phases, i.e. all the heat applied is used to evaporate the liquid. Thus, if W kg s^{-1} of saturated liquid enters a tube of length L with heat flux q, quality at exit from tube is

$$x = \frac{\pi DLq/i_{\text{fg}}}{W} \tag{1.2.15}$$

where i_{fg} is the latent heat of vaporization. Equilibrium quality during condensation is defined in a similar way; all heat removed is used to condense the vapor. Unless stated otherwise, the quality used in equations and given in test data is the equilibrium quality.

If T_w be the wall temperature and T_{SAT} the saturation temperature during boiling, $(T_w - T_{\text{SAT}}) = \Delta T_{\text{SAT}}$ is known as the wall superheat. In condensation, $(T_{\text{SAT}} - T_w)$ is called wall subcooling. If a liquid is at a temperature T that is lower than the saturation temperature, $(T_{\text{SAT}} - T) = \Delta T_{\text{SC}}$ is called subcooling.

The term "film temperature" is frequently used. It means the mean of wall and fluid temperature. Unless stated otherwise, it is the arithmetic mean. Thus,

$$T_{\text{film}} = \frac{T_{\text{wall}} + T_{\text{fluid}}}{2} \tag{1.2.16}$$

1.3 Various Models

Some basic models used in the analysis of two-phase systems are discussed herein.

1.3.1 Homogeneous Model

It is assumed that gas and liquid are flowing at the same velocity and form a homogeneous mixture. By putting $u_G = u_L$ in Eq. (1.2.8) and rearranging, the following expression for void fraction α is obtained:

$$\alpha = \left[1 + \left(\frac{1-x}{x}\right)\left(\frac{\rho_g}{\rho_f}\right)\right]^{-1} \tag{1.3.1}$$

For use in calculation of heat transfer and pressure drop with this model, the properties of the mixture are considered to be the mean of those of gas and liquid. Various methods of calculating the mean values have been proposed, for example, weighted according to the mass fractions of gas and liquid in the mixture.

Homogeneous model works fairly well for bubble flow and mist flow though it has been used in some empirical correlations without regard to the flow pattern.

1.3.2 Separated Flow Models

In the separated flow model, the gas and liquid phases are considered to be separated. Separate equations can then be written for each phase. Additional equations are needed for determining areas occupied by the two phases and interfacial shear. These can be empirical or semi-theoretical correlations or sophisticated analyses such as the two-fluid models in which momentum, energy, and continuity equations are written separately for each phase together with equations for interaction between phases. Closed-form solutions of these equations are rarely possible and hence have to be solved numerically on computers. The two-fluid models are difficult to use and not necessarily more accurate than the simpler models. Empirical and semi-theoretical models are generally used in practical designs.

1.3.3 Flow Pattern-Based Models

In these models, the gas and liquid are considered to be arranged according to the expected flow pattern, and prediction methods are developed specific to particular flow patterns. The prediction methods are most often empirical correlations. Analytical solutions have also been developed notably for stratified, slug, and annular flow patterns. Such analytical solutions use idealized geometry of the flow patterns. For example, annular flow is usually assumed to have uniform liquid layer, no interfacial waves, and no liquid entrainment. These assumptions are usually not correct. Still, the analytical solutions are useful as they provide understanding of the physical phenomena.

The accuracy of flow pattern-based models is further limited by the accuracy of flow pattern prediction methods. One of the most verified flow pattern correlation is that of Mandhane et al. (1974). They report an accuracy of 68% in prediction. Researchers often report that their observed flow patterns do not agree with well-known flow pattern correlations. For example, Kim (2000) found large differences between his own flow pattern observation in air–water flow and the predictions of the Taitel and Dukler (1976) map.

Due to the previously mentioned factors, the accuracy of flow pattern-based prediction methods is not good.

1.4 Classification of Channels

In recent years, there has been increasing use of small diameter channels known as mini- or microchannels as they offer more compact and economical heat exchangers. Most of the methods for predicting heat transfer were developed with data for larger tubes known as conventional or macro channels.

The generally held view is that there is no effect of surface tension on heat transfer in tubes of larger diameter, while in tubes of small diameter, surface tension affects heat transfer. The implication is that methods for predicting heat transfer in macro channels are not applicable to mini-/microchannels. It is therefore necessary to demarcate the boundary between macro channels and minichannels to ensure use of macro channel correlations only within their applicable range.

Many classifications of channels have been proposed. These have most recently been discussed by Shah (2018).

1.4.1 Based on Physical Dimensions

According to Shah (1986), the heat exchangers with area-to-volume ratio more than 700 m^2 m^{-3} are compact. This results in 6 mm diameter being the boundary between minichannels and macro channels.

Mehendale et al. (2000) proposed the following:

$D > 6$ mm, macro channels
$D = 1$–6 mm, compact channel
$D = 100$ μm to 1 mm, meso channel
$D = 1$–100 μm, microchannel

A widely used one is by Kandlikar (2002), according to which

Conventional channels: $D > 3$ mm
Minichannels: $3\ \text{mm} \geq D > 0.2$ mm
Microchannels: $0.2\ \text{mm} \geq D > 0.01$ mm

This classification was based mainly on single-phase flow of gases, but for uniformity, he also recommended it for boiling and condensing flows. This is the most widely used classification.

1.4.2 Based on Condensation Studies

Li and Wang (2003) studied condensation in minichannels. They observed the transition of flow patterns from symmetrical to asymmetrical and noted that these depend on the capillary length L_{cap} (also known as Laplace constant) defined as

$$L_{cap} = \left[\frac{\sigma}{g(\rho_f - \rho_g)}\right]^{0.5} \tag{1.4.1}$$

Their conclusions were as follows:

- $D < 0.224L_{cap}$: Gravity forces are negligible compared with surface tension forces. Flow regimes are symmetrical.
- $0.224L_{cap} < D < 1.75L_{cap}$: Gravity and surface tension forces are comparable. Flow distribution is slightly stratified.
- $1.75L_{cap} < D$: Gravity forces dominate surface tension forces and the flow regimes are similar to macro channels.

Cheng and Wu (2006) rearranged the preceding results of Li and Wang in terms of Bond number as follows:

Microchannel, if $Bd < 0.5$ (negligible effect of gravity)
Minichannel, if $0.5 < Bd < 3.0$ (both gravity and surface tension have significant effect)
Macro channel, if $Bd > 3.0$ (surface tension has negligible effect).

Bond number is the ratio of surface tension and gravitational forces and is defined as

$$Bd = \frac{gD^2(\rho_f - \rho_g)}{\sigma} \tag{1.4.2}$$

It is also the ratio of channel diameter to capillary length.

Based on the comparison of his general correlation for condensation in tubes, Shah (2009, 2013), with a wide-ranging database, Shah (2016) gave the following criterion. It is minichannel if

$$We_{\mathrm{GT}} < 100 \tag{1.4.3}$$

where

$$We_{\mathrm{GT}} = \frac{G^2 D}{\rho_G \sigma} \tag{1.4.4}$$

The data for $We_{\mathrm{GT}} < 100$ included Bond numbers up to 105. Hence the criteria based on Bond number were found to be incorrect as they consider effect of surface tension to occur at Bond numbers between 1 and 4.

1.4.3 Based on Boiling Flow Studies

The growth of bubbles during boiling in small channels may be restricted due to the limitation of tube diameter. This has led several authors to use the confinement number Co defined as

$$Co = \frac{1}{D}\left[\frac{\sigma}{g(\rho_f - \rho_g)}\right]^{0.5} \tag{1.4.5}$$

Kew and Cornwell (1997) compared the data from their tests on heat transfer during boiling in tubes of diameter 1.39, 2.87, and 3.69 mm, and a square channel 2 mm × 2 mm, to several correlations based on macro channel data. They found that these failed when the confinement number Co is less than 0.5. Accordingly, they gave the following classification:

Micro-/minichannel: $Co > 0.5$
Macro channel: $Co < 0.5$

According to Ong and Thome (2011a), the lower threshold of macroscale flow is Co = 0.3–0.4, while the upper threshold of symmetric microscale flow is Co = 1 with a transition (or mesoscale) region in between. This was based on the experimental two-phase flow pattern transition data together with a top/bottom liquid film thickness comparison for refrigerants R-134a, R-236fa, and R-245fa during flow boiling in channels of 1.03, 2.20, and 3.04 mm diameter.

Li and Wu (2010a,b) have given a transition criterion based on their analysis of data for boiling heat transfer in a variety of channels. According to it, it is minichannel if

$$Bd\, Re_{\mathrm{LS}}^{0.5} \le 200 \tag{1.4.6}$$

Shah (2017b) compared a very wide-ranging database for saturated boiling prior to CHF with several correlations for macro channels including Shah (1982). He concluded that it is minichannel if

$$F = (2.1 - 0.008 We_{\mathrm{GT}} - 110 Bo) > 1 \tag{1.4.7}$$

Bo is the boiling number. For horizontal channels, $F = 1$ if $Fr_{\mathrm{LT}} < 0.01$. If $F \le 1$, it is macro channel. The data for $F > 1$ (minichannel) included diameters up to 6.4 mm and Bd up to 13.7. The data for $F \le 1$ (macro channels) include diameters down to 0.38 mm and Bond numbers down to 0.15. Hence the criteria based on Bond number and diameter are not satisfactory

Shah (2017a) compared his general correlation for subcooled boiling in tubes and annuli with a wide-ranging database that included diameters as small as 0.176 mm and Bond number down to 0.025. Data over the entire range were satisfactorily predicted. This correlation did not include any factor for surface tension effects. No effect of diameter or Bond number was found.

Shah (2017c) compared his correlation for dispersed flow film boiling in horizontal and vertical tubes with a wide-ranging database. This correlation did not have any factors for surface tension effects. Data over the entire range were satisfactorily predicted. These included tube diameters as low as 0.98 mm and Bond numbers down to 2. The minimum We_{GT} in these data was 32. This shows that the Shah criterion for saturated boiling, Eq. (1.4.7), does not apply to film boiling.

Shah (2015, 2017d) compared his correlation for CHF in vertical and horizontal tubes with a very wide range of data. These correlations had no factors for the effect of surface tension. The data included diameters down to 0.13 mm and Bond numbers down to 0.026. The minimum We_{GT} in the data was 6. Hence the criterion of Eq. (1.4.7) for saturated boiling heat transfer is not applicable to CHF.

1.4.4 Based on Two-Component Flow

Triplett et al. (1999) studied gas–liquid flow in small diameter channels. They proposed that mini-/microchannels are those with diameter less than capillary length L_{cap}. This is equivalent to $Bd < 1$.

Ullmann and Brauner (2007) studied flow pattern transitions in gas–liquid flow in channels, and based on their analyses, they proposed that the transition between minichannels and macro channels depends on the Eotvos number Eo, which is the ratio of buoyancy force to surface tension force. It is written as

$$Eo = \frac{g(\rho_{f-}\rho_g)D^2}{8\sigma} \tag{1.4.8}$$

They proposed that minichannels are those with $Eo < 0.2$.

1.4.5 Discussion

The criteria given earlier are summarized in Table 1.4.1. To make the comparison easy, the criteria using Eo and Co have been given in terms of Bond number. These are related by the following equation:

$$Eo = \frac{Bd}{8} = \frac{1}{8Co^2} \tag{1.4.9}$$

It is seen that the value of the transition Bond number in various criteria varies from 1 to 4. As seen in the discussion earlier, many data for condensation and saturated boiling show effect of surface tension at much higher Bond numbers, while some data at lower Bond numbers do not show effect of surface tension. Hence the criteria based on Bond number are inaccurate. Similarly, many data for tube diameters smaller than 3 mm showed satisfactory agreement with macro channel correlations for saturated boiling and condensation, while many data for larger diameters showed effect of surface tension. Hence the limit of applicability of macro channel correlations to minichannels cannot be based on criteria based on tube diameter or Bond number. For saturated boiling and condensation, the criteria given by Shah are well verified. For subcooled boiling, film boiling, and CHF, limits of applicability of macrochannel correlations are as yet unknown.

1.4.6 Recommendation

Distinction has to be made between naming convention and the actual boundary according to the limit of applicability of macro channel correlations.

In most literature, channels with diameter > 3 mm are called conventional or macro channels, while those with diameter ≤ 3 mm are called minichannels. Hence this naming convention is also followed in this book. However, this is not the limit of applicability of macro channel correlations. The following are the recommendations for this limit:

- For condensation heat transfer, Shah's criterion $We_{GT} > 100$.
- For saturated boiling heat transfer, Shah's Eq. (1.4.7).
- For subcooled boiling, film boiling, and CHF, the limit is undefined. Use macro channel correlations within the range of data in the analyses of such data performed by Shah (2017a,c,d).

1.5 Flow Patterns in Channels

1.5.1 Horizontal Channels

1.5.1.1 Description of Flow Patterns

There is a great deal of variation in the description and names of flow patterns used by different authors. Rouhani

Table 1.4.1 Criteria for macro to mini transition by various authors.

Author	Criterion for minichannel	Basis
Shah (1986)	$D < 6$ mm	Surface-area-to-volume ratio > 700 m^2 m^{-3}
Mehendale et al. (2000)	$D < 6$ mm	Same as above
Kandlikar (2002)	$D \leq 3$ mm	Based on mean free path of common gases
Kew and Cornwell (1997)	$Bd < 4$	Bubble growth confinement during boiling in channels
Triplett et al. (1999)	$Bd < 1$	Flow pattern transitions in gas–liquid flows
Ullman and Brauner (2007)	$Bd < 1.6$	Flow pattern transitions in adiabatic gas–liquid flows
Cheng and Wu (2006)	$Bd < 3$	Flow pattern transitions during condensation in tubes
Ong and Thome (2011a)	$Bd < 1$	Flow pattern transitions and top-bottom liquid film thickness during boiling in channels
Li and Wu (2010aa,b)	$Bd \cdot Re_{LS}{}^{0.5} \leq 200$	Correlation of heat transfer coefficients during saturated boiling in channels
Shah (2016)	$We_{GT} < 100$	Comparison of test data with correlation for condensation heat transfer in macro channels
Shah (2017b)	$F = (2.1 - 0.008We_{GT} - 110Bo) > 1$	Comparison of test data with correlation for saturated boiling heat transfer in macro channels

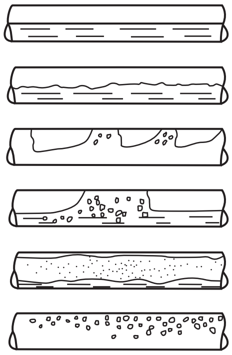

Figure 1.5.1 Flow patterns during co-current gas–liquid flow in horizontal tubes. Source: From Rouhani and Sohal (1983). © 1983 Elsevier.

and Sohal (1983) note that there are 84 different flow pattern labels in literature, 60 of them being for horizontal co-current flow. The most common names are used herein.

Typical flow patterns occurring during flow of gas–liquid mixtures in horizontal channels are shown in Figure 1.5.1. Flow in horizontal channels is subjected to gravity, inertia, and surface tension forces, and the flow patterns result from the balance of these forces. Gravity force tends to pull the heavier liquid phase to the bottom, while the inertia force tends to keep the flow symmetrical. At low flow rates, stratified flow occurs in which the liquid flows at the bottom, while gas flows at the top. The interface is smooth at the lowest flow rates. As flow rates increase, gas–liquid interface becomes rough with appearance of ripples and waves. This is usually called the stratified-wavy pattern. If the waves are of significant height, many authors call it the wavy pattern. With further increase in flow rates, the wave amplitude increases and they reach the top of tube. Gas pockets/plugs then get trapped between the liquid crests, resulting in the plug and slug flow regimes. The difference between plug and slug patterns is mainly that gas pockets are larger in slug flow. Slug flow is often called Taylor flow. Plug and slug flow are also called intermittent flow. Considerable pressure fluctuations occur during intermittent flow. As gas and liquid flow rates increase further, the annular flow pattern occurs. The churn flow pattern may occur in transition from slug flow to annular flow as the slugs begin to disintegrate. In annular flow, liquid is in the form of a layer around the tube circumference, and gas flows in the middle of the tube. Considerable amounts of liquid drops may be entrained in the vapor core and interfacial waves occur. If the liquid layer is thin or non-existent at the upper part of tube, some authors call it semi-annular or crescent pattern. This pattern often occurs during evaporation in tubes. At high gas/vapor velocities, large amount of liquid is torn off the liquid film, and the gas core carries large amounts of liquid droplets. This is called the mist-annular flow; it is called mist flow if there is no liquid film. During dispersed bubble flow (also called bubble flow), vapor bubbles are carried in the continuous liquid stream. It occurs at high liquid flow rates together with low gas flow rate.

Figure 1.5.2 shows the flow patterns during evaporation in horizontal tubes under two conditions common in refrigeration evaporators.

1.5.1.2 Flow Pattern Maps

Many maps for prediction of flow patterns have been proposed. One of the best known is that of Baker (1954). The original map was in terms of dimensional parameters. Figure 1.5.3 is an essentially dimensionless version. This map was developed by analysis of mostly air–water data in pipes of diameters up to 50 mm. G_l and G_g are the superficial mass velocities of liquid and gas. The other terms are

$$\lambda = \left(\frac{\rho_g}{\rho_{\text{air}}} \frac{\rho_f}{\rho_{\text{water}}} \right)^{0.5} \tag{1.5.1}$$

$$\phi = \left(\frac{\sigma_{\text{water}}}{\sigma} \right) \left[\frac{\mu_f}{\mu_{\text{water}}} \left(\frac{\rho_{\text{water}}}{\rho_f} \right)^2 \right]^{1/3} \tag{1.5.2}$$

The subscripts “air” and “water” indicate air and water at room temperature and pressure. While this map was based entirely on adiabatic flow, several authors have reported its agreement with boiling and condensation data. For example, Shah (1975) reported it to be in fairly good agreement with his data for ammonia evaporating in a 26.2 mm diameter pipe.

A well-verified correlation is by Mandhane et al. (1974) shown in Figure 1.5.4. It was developed using adiabatic gas–liquid data for many gas–liquid combinations. The range of those data is given in Table 1.5.1. Its success in correctly predicting the flow patterns was 67.1%. For the same data, Baker map was able to correctly predict only 41.5% of them. Other researchers have generally found it to be fairly good. Mandhane et al. have also given a version that includes fluid properties but its accuracy was about the same as that of this simple version. They have given a computer subroutine for this correlation.

Another widely quoted flow pattern map is that of Taitel and Dukler (1976). It was developed analytically. Kim (2000) found large differences between his own flow pattern observation in air–water flow and the predictions of the Taitel and Dukler (1976) map.

A number of maps have been developed specifically for boiling and condensation. Among them are those of El Hajal et al. (2003) for condensation and Kattan et al. (1998) for boiling. These were verified with data for halocarbon refrigerants.

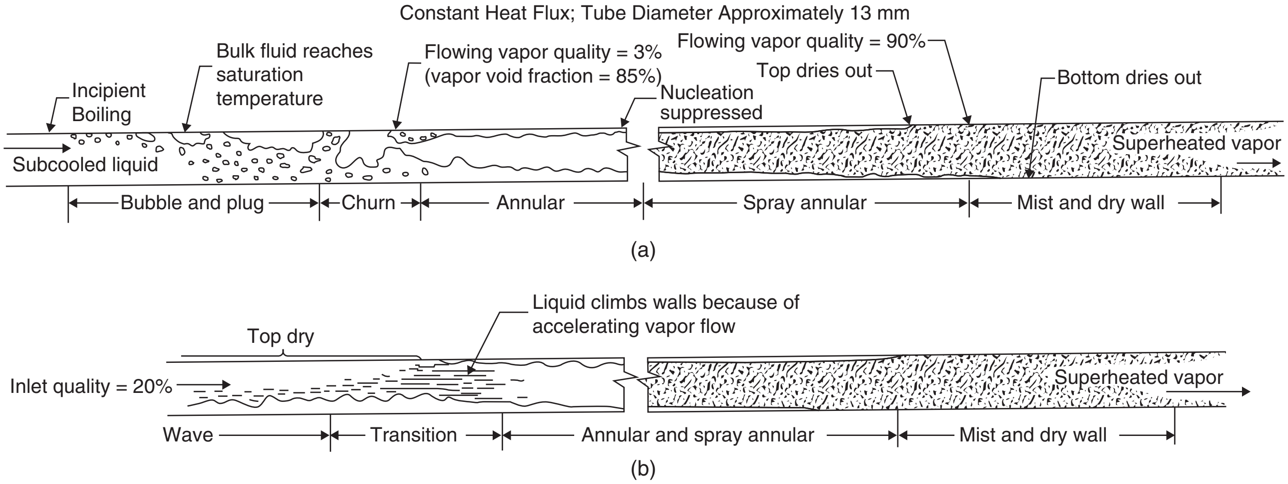

Figure 1.5.2 Flow patterns during evaporation in horizontal tubes. (a) High mass velocity (400 kg s^{-1} m^{-2}), subcooled liquid at inlet. (b) Low mass velocity (200 kg s^{-1} m^{-2}), 20% flash gas at inlet. Source: From ASHRAE (2017).

Figure 1.5.3 Baker flow pattern map for co-current gas–liquid flow in horizontal pipes. Source: From Rouhani and Sohal (1983). © 1983 Elsevier.

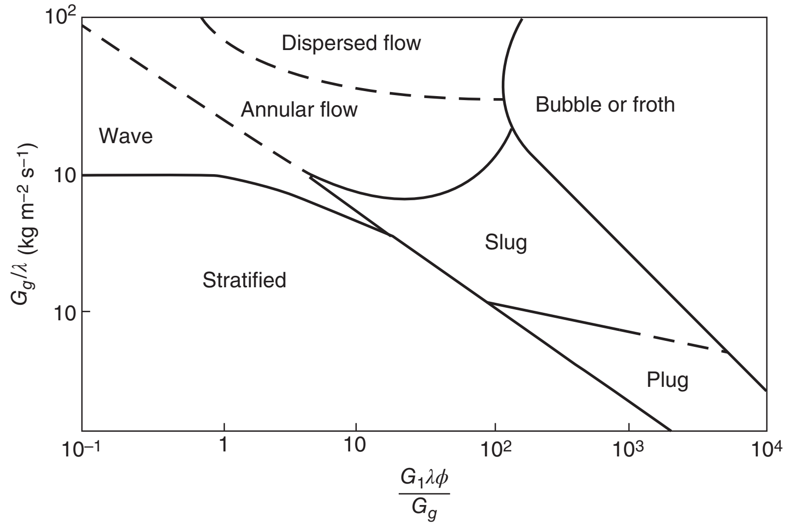

1.5.2 Vertical Channels

Figure 1.5.5 shows the most common flow patterns in vertical upward co-current flow. These are mostly similar to the horizontal flow patterns except that they are more axisymmetric and the stratified pattern does not occur. This is because gravity force is parallel to the flow direction.

An early flow pattern map is by Hewitt and Roberts (1969), which was based on steam–water flow. Mishima and Ishii (1984) analytically developed criteria for transitions between flow patterns. These were compared to data for air–water and boiling water in round and rectangular channels from several sources and found to be in fair agreement with them. Flow pattern maps can be drawn for any conditions using these criteria. Figure 1.5.6 shows their predicted map for air–water flow at room conditions in a 25.4 mm pipe. In the Region A shown in it, it is difficult to distinguish between churn and annular flow as it is highly agitated.

McQuillan and Whalley (1985) analytically derived criteria for transitions between flow patterns in co-current upflow. Figure 1.5.7 is an example of their predictions. They compared their map with data for air–water as well as for boiling water and refrigerants. Agreement was generally good with 84.1% of the data points predicted correctly.

1.5.3 Inclined Channels

By inclined channels is meant channels with flow directions other than horizontal and vertical up.

The flow patterns in different inclinations change due to the changing relative direction of gravitational force. Analytical expressions for transition criteria have been developed by several authors for particular flow directions.

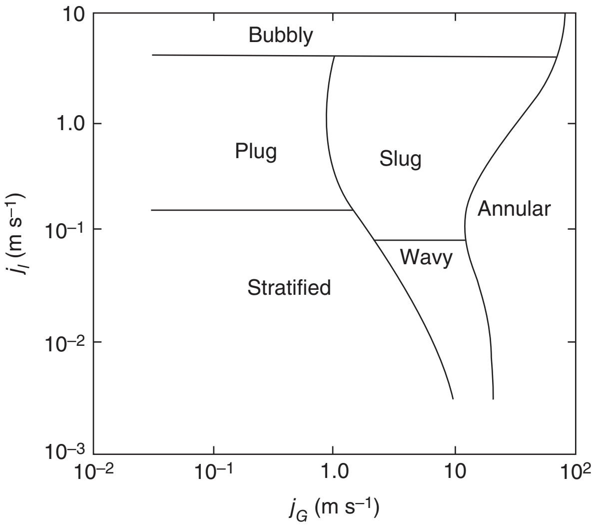

Figure 1.5.4 The Mandhane et al. flow pattern map for co-current flow in horizontal pipes. Source: From Ghiaasiaan et al. and Cambridge University Press. © 1974 Elsevier.

Table 1.5.1 Range of data with which flow pattern map of Mandhane et al. was verified.

	Range
Pipe diameter (mm)	12.7–165.1
Liquid density (kg m^{-3})	705–1009
Gas density (kg m^{-3})	0.8–50.5
Liquid viscosity (Pa s)	3×10^{-4}–9×10^{-2}
Gas viscosity (Pa s)	10^{-5}–2.2×10^{-5}
Surface tension (N m^{-1})	0.024–0.103
Superficial liquid velocity (m s^{-1})	0.9×10^{-3}–7.3
Superficial gas velocity (m s^{-1})	0.04–171

Source: Modified from Mandhane et al. (1974).

Barnea (1987) developed a comprehensive model that is applicable to all flow directions from vertical up to vertical down. It consists of equations for transitions between flow patterns. Figure 1.5.8 shows their predicted flow patterns over the entire range of inclinations from vertical up to vertical down. Good agreement with data from one source is seen. Data from the same source for a 25 mm pipe also showed good agreement. Comparison of this model with data from many sources covering a wide range of parameters is needed.

Mehta and Banerjee (2014) observed flow patterns during air–water flow in a 2.1 mm diameter tube whose orientation was varied at various angle from vertical up to vertical down. They compared their observations with several flow pattern maps, but none was found to agree with their data. They developed maps for horizontal, vertical upflow, and vertical downflows, which were verified only with their own data.

1.5.4 Annuli

Kelessidis and Dukler (1989) investigated flow patterns in vertical upward gas–liquid flow in a concentric and an eccentric annulus (eccentricity 50%). Flow patterns observed were essentially the same as in tubes. Eccentricity was found to have only minor effect on flow patterns. They derived expressions for transitions between flow patterns. These were found to be in agreement with their own data.

Das et al. (1999a,b) observed flow patterns during adiabatic gas–liquid upflow in vertical annuli and developed a mechanistic model of the flow pattern transitions that agreed with their data.

Julia and Hibiki (2011) developed criteria for transitions between flow patterns during upflow in annuli. They compared their map with adiabatic data mentioned earlier as well as boiling water data of Hernandez et al. (2010). Satisfactory agreement was found.

1.5.5 Minichannels

All the foregoing discussions were on flow patterns in macro/conventional channels. Those in minichannels are addressed in this section.

Numerous experimental studies have been done on flow patterns in minichannels, and many flow pattern maps have been proposed. Cheng et al. (2008) reviewed many of them. Experimental studies show that flow patterns in minichannels are the same as in macro channels, but criteria for transitions between flow patterns are usually different.

Triplett et al. (1999) studied flow patterns during air–water flow in horizontal tubes of diameter 1.09 and 1.49 mm. They compared their data to some macro channel maps and found them unsatisfactory.

Akbar et al. (2002, 2003) studied data for air–water in horizontal and vertical minichannels from six sources and proposed a new flow pattern map.

Chen et al. (2006) performed tests with R-134 boiling with upward flow in vertical tubes of diameter 1.10, 2.01, 2.88, and 4.26 mm. They found the Akbar et al. (2003) map unsatisfactory for their data. They noticed subtle differences between the flow patterns of the two larger tubes and the two smaller tubes. The smaller tubes had slimmer vapor slugs and thinner liquid films around the vapor slugs, suggesting greater influence of surface tension. They therefore considered $D = 2$ mm as the boundary between minichannels and macro channels for the conditions of their tests.

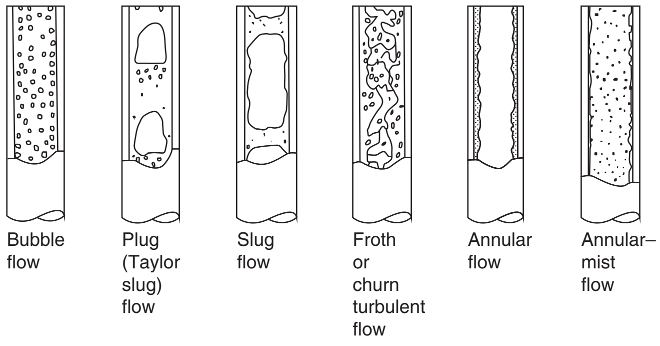

Figure 1.5.5 Flow patterns during upflow in vertical pipes. Source: From Rouhani and Sohal (1983). © 1983 Elsevier.

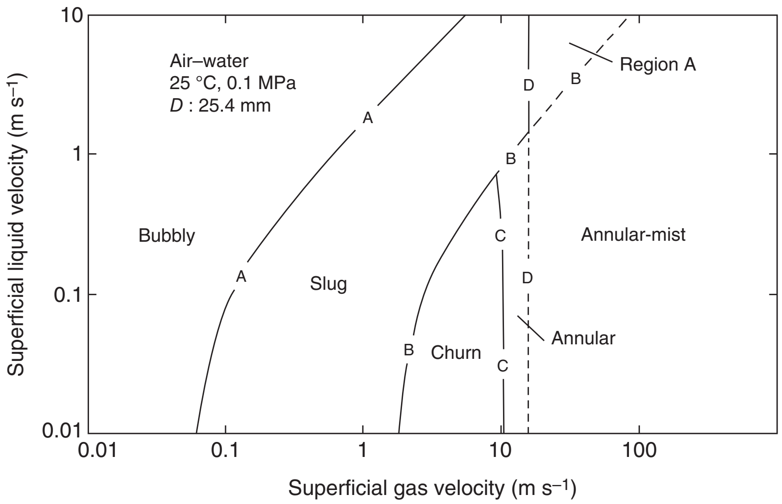

Figure 1.5.6 Example of flow patterns according to the transition criteria of Mishima and Ishii. Source: From Mishima and Ishii (1984). © 1984 Elsevier.

Ullmann and Brauner (2007) analytically developed criteria for transition between flow patterns. They concluded that for flow patterns, transition between minichannel and macro channel occurs at Eotvos number of 0.2. They compared their map with the flow patterns observed by Triplett et al. (1999) in a 1 mm diameter tube with air–water flow. Satisfactory agreement was found.

Ong and Thome (2011b) studied boiling of three refrigerants in tubes of diameter 1.03, 2.20, and 3.04 mm. They gave a new flow pattern map that agreed with their data. Saisorn et al. (2018) found satisfactory agreement with this map of their data for R-134 boiling in a 1 mm diameter tube in horizontal, vertical upflow, and vertical downflow.

Jige et al. (2018) experimentally investigated R-32 boiling in horizontal multiport rectangular minichannels with hydraulic diameters of 0.5 and 1.0 mm. Mass velocity range was 30–400 kg m^{-2} s^{-1} at a saturation temperature of 15 °C. They compared their observations with flow pattern transition criteria of Garimella et al. (2002) and Enoki et al. (2013), both for minichannels. Agreement was not good. They developed their own map.

As is evident from the earlier discussions, many flow pattern maps for minichannels have been proposed, but none of them has been verified with a wide range of data.

1.5.6 Horizontal Tube Bundles with Crossflow

A number of experimental studies have been done on upflow across horizontal tube bundles. Most of them were done with air–water, while a few were with boiling and condensation. Flow patterns observed included bubble, slug, churn, and annular. Xu et al. (1998) studied both downflow and upflow of air–water. In downflow, they also noticed a falling film flow pattern. This occurred at low superficial velocities of gas and liquid. The liquid formed a film around tube wall and flowed down on the tube below. Their observations during upflow and downflow are shown in Figure 1.5.9.

Flow pattern maps have been proposed by Grant and Chisholm (1979), Pettigrew et al. (1989), Ulbrich and Mewes (1994), Xu et al. (1998), Aprin et al. (2007), and Kanizawa and Ribatski (2016). All of them are based on air–water data except that of Aprin et al., which was based on their own boiling data.

Xu et al. (1998) compared their upflow data with the maps of Ulbrich and Mewes (1994) and Grant and Chisholm (1979). Significant differences were found.

Kanizawa and Ribatski (2016) performed tests with air–water flowing up across a bundle of 19 mm tubes on an

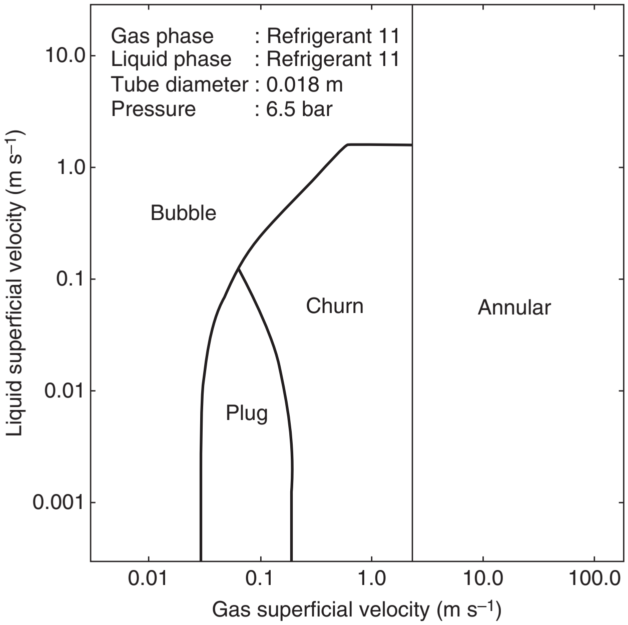

Figure 1.5.7 Flow patterns predictions of McQuillan and Whalley for evaporating R-11 during upflow in a vertical tube under the conditions shown. Source: From McQuillan and Whalley (1985). © 1985 Elsevier.

equilateral triangular arrangement. They compared their data with the maps of Xu et al. (1998), Ulbrich and Mewes (1994), and Grant and Chisholm (1979). These were able to correctly predict 48%, 69%, and 58% of the flow patterns, respectively. They developed their own flow pattern map, which agrees well with their own data.

1.5.7 Vertical Tube Bundles

Vertical tube/rod bundles are especially of interest due to their use in light water nuclear reactors in normal and post-accident conditions. A number of studies on flow patterns in such bundles have been done.

Williams and Peterson (1978) studied upflow of high pressure boiling water in a bundle consisting of a single row of four 6.35 mm rods. The observed two-phase flow patterns were bubble flow, froth flow, slug flow, and annular flow.

Venkateswararao et al. (1982) performed an experiment of vertical adiabatic air–water flow in a rod bundle under atmospheric pressure. There were 24 rods arranged on a square pitch in a cylindrical shell with 12.7 mm outside diameter and 17.5 mm pitch. They identified five flow patterns. These are bubbly, finely dispersed bubbly, slug, churn, and annular. They proposed an analytically based flow pattern map that agreed with their data.

Mizutani et al. (2007) also studied air–water upflow in a 4 × 4 bundle of 12 mm rods with pitch of 16 mm. They identified the following flow patterns: bubbly, bubbly–churn, churn, churn–annular, and annular flows. They developed a map that agreed well with their own data.

Paranjape et al. (2011) had air–water flowing up an 8 × 8 bundle of 12.7 mm diameter rods with square arrangement and a pitch of 16.7 mm. They observed four flow patterns, namely, bubbly, cap-bubbly, cap-turbulent, and churn–turbulent flows. Cap-bubbly indicates that the bubbles were cap shaped. A map of their flow patterns was presented.

Zhou et al. (2015) studied vertical boiling steam–water flow in a 3 × 3 heated rod bundle at atmospheric pressure. The rods were 10 mm diameter at 15 mm square pitch. The flow patterns observed were bubbly, bubbly–churn, churn, and annular. They also proposed a map that agreed with their data.

Liu and Hibiki (2017) showed that the flow pattern maps mentioned earlier do not agree well with data other than their own. Liu and Hibiki analytically developed their own flow pattern map that identifies six flow patterns. It was shown to be in fair agreement with data of Zhou et al. (2015), Paranjape et al. (2011), Mizutani et al. (2007), and Venkateswararao et al. (1982). They did not compare it with the data of Williams and Peterson (1978).

1.5.8 Effect of Low Gravity

All the foregoing discussions were for systems operating under Earth gravity. Flow patterns under micro gravity (<0.03 Earth gravity) condition are addressed herein.

Experimental studies show that flow patterns in microgravity are the same as under Earth gravity but the transitions between flow patterns are different.

The earliest experimental study at near-zero gravity was by Heppner et al. (1975). They used air–water in 25.4 mm diameter tube. They compared the observed flow pattern transitions to those at Earth gravity and found large differences.

Dukler et al. (1988) performed tests under microgravity conditions in a drop tower as well as in parabolic flights with air–water flowing in horizontal tubes of diameter 9.5 and 12.7 mm. Study of their data and analysis led them to the following criteria for transitions between flow patterns:

$$\text{Bubble to slug,}\quad u_{LS} = 1.2\,u_{GS} \tag{1.5.3}$$

$$\text{Slug to annular,}\quad \frac{u_{GS}}{u_{LS} + u_{GS}} = C_0 \tag{1.5.4}$$

Study of their data showed C_0 between 1.15 and 1.3. They tentatively chose a value of 1.25. Rezkallah (1990) found these criteria to be in fair agreement with data from several sources as seen in Figure 1.5.10. The data of Hill et al. (1987) were for Freon 114 boiling in a 15.8 mm diameter tube. In